

in appearance from that of the complex. The equatorial scattering in the small-angle X-ray photograph of the polymer is more intense than that of the complex. This feature may support the increment of microvoids parallel to the fiber axis. On the other hand, no distinct scattering along the meridian is found in either of the photographs. These facts suggest that the polymer chains aggregate and crystallize without "chain folding," at least without "regular chain folding," upon removal of thiourea.

In conclusion, the canal polymerizations of 2,3-dichlorobutadiene and 2,3-dimethylbutadiene are analogous from a structural viewpoint. The thiourea canal structures of both the monomer-thiourea complexes are considerably deformed from a regular hexagonal prism. Such a deformation of the canals is favorable for inclusion of the guest molecules and also for 1,4-trans tactic polymerization. Though there is too little information about the structures of canal complexes to permit generalizations concerning the specificity of canal

polymerization, the following conclusions are permissible. (1) The shape of thiourea canal is adaptable to some extent, depending upon the size and shape of guest molecule so long as intermolecular N...S distances of 3.4–3.5 Å are maintained. (2) If a resultant polymer chain cannot assume a suitable shape and/or size for the original canal, the complex may be degraded by polymerization, and polymer yield may be limited. (3) The canal does exert a spatial control which can promote polymerization, and in a special case, such as the trioxecane-urea complex, a chemical control for polymerization (inhibition of polymerization) is also possible.

**Acknowledgment.** The authors wish to thank Professor H. Tadokoro for his interest in the work and his constant encouragement and also Dr. T. Mochizuki of Kuraray Co. Ltd. for preparation of the scanning electron microscopic photographs. The authors also wish to acknowledge the hospitality of the Radiation Laboratory of Osaka University.

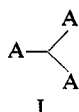
## Angular Distribution of Rayleigh Scattering from Branched Polycondensates. Amylopectin and Glycogen Types

Walther Burchard

*Institute of Macromolecular Chemistry, University of Freiburg, 78 Freiburg i. Br., West Germany. Received May 5, 1972*

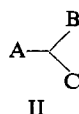
**ABSTRACT:** The polycondensation of trifunctional monomers with groups A, B, and C of different reactivities is considered under the restriction that group A can react only with either group B or C. This condensation leads to polymers of the branched structure of amylopectin and glycogen with no possibility of gel formation. Simple formulas for the weight and number averages of the degree of polymerization and for the  $z$  averages of the mean-square radius of gyration and of the particle scattering factor are derived with the aid of the cascade theory developed by Good and by Gordon. For large  $DP_w$ , the mean-square radius of gyration ( $S^2$ ), is found to increase proportionally with the square root of the weight-average degree of polymerization but linearly with the number average. This behavior is interpreted in terms of the heterogeneity which at large  $DP_w$  is  $DP_w/DP_n \cong DP_w^{1/2} \cong DP_n$ . The Zimm plots of the particle scattering factor exhibit significant upturns. This behavior deviates from the linear Zimm plots of the particle scattering factors of randomly branched polycondensates, and it is explained by the considerably narrower molecular weight distributions compared with the random cases.

In a previous paper Kajiware, Burchard, and Gordon<sup>1</sup> reported a new method for the calculation of the particle scattering factor of randomly branched polycondensates in which the simple case of homopolymers built up from  $f$ -functional monomers was treated. For example, when  $f = 3$  such a monomer can be represented by



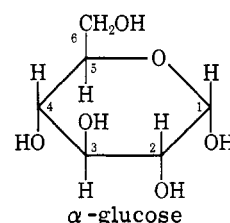
where each of the A groups has equal probability of reaction with any other unreacted A group of another molecule.

A consequent extension of such a reaction is the consideration of monomers of the type



where A, B, and C have different reactivities. In this paper branched polymers which are formed by the condensation of this type of monomer will be treated, but with the restriction that group A can react only with either group B or C, and that all other conceivable possibilities are excluded.

This type of condensation has some biological significance, because the branching of saccharides resulting in glycogen, amylopectin, and dextran is of this kind. In these polysaccharides the three groups A, B, and C are respectively in the C1, C4, and C6 positions on the glucose ring, A is an aldehydic OH group, and B and C are alcoholic groups.



(1) K. Kajiware, W. Burchard, and M. Gordon, *Brit. Polym. J.*, **2**, 110 (1970).

Two sorts of  $\alpha$ -glycosidic bonds (*i.e.*, C1–C4 and C1–C6) can

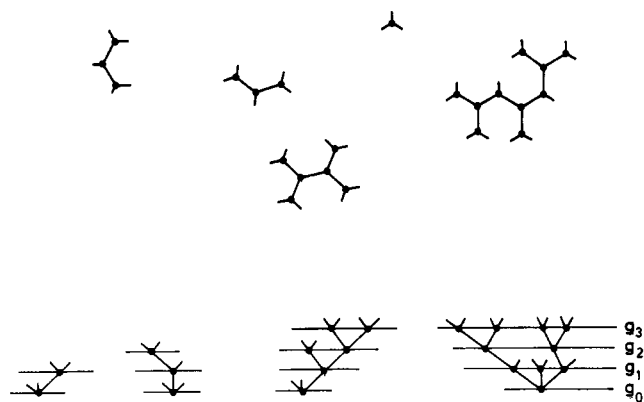


Figure 1. Molecular assembly of branched molecules and the corresponding forest of rooted trees.

be formed with different frequencies under the action of two enzymes.

The formation of  $\alpha$  C1–C4 bonds is found to be 4 and 12 times more frequent in glycogen and amylopectin, respectively, than the formation of  $\alpha$  C1–C6 bonds, while the situation is opposite for dextran, where the  $\alpha$  C1–C6 bond is about 12 times more frequent than the  $\alpha$  C1–C4 bond.

The type of condensation shown above as II was first considered by Erlander and French.<sup>2</sup> They applied a method of calculation developed by Flory<sup>3</sup> and succeeded in the calculation of the molecular weight averages  $M_n$ ,  $M_w$ , and  $M_z$ .

Here details of calculation of some conformational averages are given, for example, the  $z$  average of the mean-square radius of gyration and the  $z$  average of the particle scattering factor. The results of Erlander and French are also obtained, as a by-product.

### Theory

The basis of the calculation is the theory of cascade processes developed by Good<sup>4</sup> and by Gordon.<sup>5–7</sup> As this method is not very familiar to chemists, a brief outline will be given which will not be strict from the mathematical standpoint but may give insight in the power of the method.

**General Considerations.** Consider an assembly of branched molecules as symbolized in Figure 1 (top). If a chain element (repeat unit) of a molecule is chosen at random and put as a root, one obtains trees, as shown by Figure 1 (bottom). The nodes correspond to the centers of a unit and the edges to the functionalities of the unit. The size of such a tree could be calculated by counting the nodes in the different generations, starting with the root as the zeroth generation, and summing. However, since each unit of a molecule in the assembly of Figure 1 has the same chance of being a root of a tree, one has to consider not only one special tree but the whole forest consisting of all possible rooted trees. For instance, there are six possible different rooted trees for the hexamer given in Figure 2 (shown in the bottom part of Figure 2).

Let  $N_{xk}$  be the frequency of a special isomer  $k$  of degree of polymerization  $x$ . The average size of a tree from the mo-

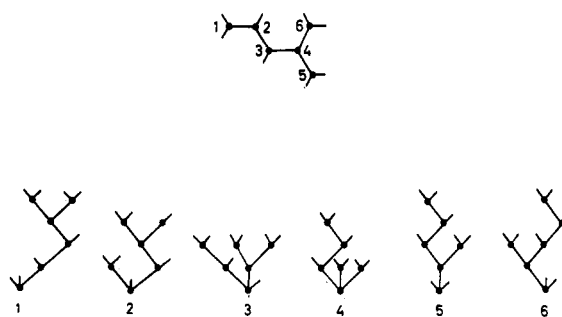


Figure 2. The six possible rooted trees of a special hexamer.

lecular assembly of Figure 1 is then, by inspection, the weight-average degree of polymerization, because there are  $xN_{xk} \propto w_{xk}$  possible rooted trees for each isomer of the degree of polymerization  $x$ ;  $w_{xk}$  is thereby the weight fraction of the  $k$ th isomer of molecules in the assembly. Instead of simply counting the nodes in the different generations, one can provide the nodes with a weighting factor  $\phi(n)$  depending on the generations or on the path length of a node in the  $n$ th generation from the zeroth generation. Typical representatives of such weighting functions are<sup>1</sup>

$$\phi(n) = M_0 \quad (1a)$$

$$\phi(n) = \sigma^2 n \quad (1b)$$

$$\phi(n) = \left\langle \frac{\sin hr_n}{hr_n} \right\rangle = \exp\left(\frac{-h^2\sigma^2}{6} n\right) \quad (1c)$$

where  $M_0$  = molecular weight of a unit and  $\sigma$  = effective bond length. Functions of (1b) and (1c) are encountered in the calculation of the mean-square radius of gyration and the particle scattering factor of gaussian chains.<sup>8</sup> Evidently, the sum of all possible path lengths is correlated to conformational averages.

Thus, the main problem is how to count trees. Good and later Gordon showed that the use of generating functions leads to relatively simple and easily accessible results for this formidable looking statistical problem.

**Probability of Offspring.** Gordon made use of Flory's concept<sup>7</sup> that all molecular averages of a branched polymer must be correlated to the extent of reaction, *i.e.*, the fraction of a special type of reactive groups which may have been reacted. Let  $\alpha_a$ ,  $\alpha_b$ , and  $\alpha_c$  be the probabilities (extent of reaction) for a reaction of the groups A, B, and C in the monomer II. One now wishes to know for given values of  $\alpha_a$ ,  $\alpha_b$ , and  $\alpha_c$ , the average-number of offspring for a monomer in the zero, the first and all other generations. Mathematically the answer is found by convolution of the three-link probability distributions  $f_a$ ,  $f_b$ , and  $f_c$  of the groups A, B, and C.

$$f_0 = f_a * f_b * f_c \quad (2)$$

where  $f_0$  is the probability distribution for offspring in the zeroth generation and the asterisks stand for convolution.

The distributions  $f_b$  and  $f_c$  are very simple and have only two elements, *i.e.*,  $\alpha_b$ ,  $1 - \alpha_b$ , and  $\alpha_c$ ,  $1 - \alpha_c$ , because there are only the possibilities that B or C may have reacted or not. The third distribution  $f_a$  has three elements as A can have reacted with B or with C or not at all.

The convolution is a rather complicated process if per-

(2) S. R. Erlander and D. French, *J. Polym. Sci.*, **20**, 7 (1956).  
 (3) P. J. Flory, *J. Amer. Chem. Soc.*, **74**, 2718 (1952); "Principles of Polymer Chemistry," Cornell University Press, Ithaca, N. Y., 1953.  
 (4) (a) I. J. Good, *Proc. Camb. Phil. Soc.*, **45**, 310 (1948); (b) *ibid.*, **56**, 367 (1960); (c) *Proc. Roy. Soc., Ser. A*, **272**, 240 (1963).  
 (5) M. Gordon, *ibid.*, **268**, 240 (1962).  
 (6) G. R. Dobson and M. Gordon, *J. Chem. Phys.*, **41**, 2389 (1964).  
 (7) D. S. Butler, M. Gordon, and G. N. Malcolm, *Proc. Roy. Soc., Ser. A*, **295**, 29 (1966).

(8) P. Debye, Rubber Reserve Company Technical Report No. 637, 1945 (see D. McIntyre and F. Gormich, "Light Scattering from Dilute Polymer Solutions," Gordon and Breech, London, 1964).

formed directly, but the solution can be simplified by the use of generating functions. Then the convolution is replaced by a simple product of the generating functions  $F_a$ ,  $F_b$ , and  $F_c$

$$F_0(\theta) = F_a(\theta)F_b(\theta)F_c(\theta) \quad (3)$$

where by definition of a generating function

$$F_0(\theta) = \sum_{i=0}^{\infty} f_{0i} \theta^i \quad (4)$$

The elements of the offspring probability  $f_{0i}$  are therefore found as coefficients of the auxiliary variable  $\theta^i$  in the Taylor expansion of the generating function. Furthermore, the mean number of offspring is found by differentiation of  $F_0(\theta)$  with respect of  $\theta$  at  $\theta = 1$

$$\text{mean number of offspring} = \left. \frac{\partial F_0(\theta)}{\partial \theta} \right|_{\theta=1} = \sum_{i=1}^{\infty} i f_{0i} \quad (5)$$

The generating functions  $F_a(\theta)$ ,  $F_b(\theta)$ ,  $F_c(\theta)$  are easily set up

$$F_a(\theta) = (1 - \alpha_a + p\alpha_a\theta_B + (1 - p)\alpha_a\theta_C) \quad (6a)$$

$$F_b(\theta) = (1 - \alpha_b + \alpha_b\theta_A) \quad (6b)$$

$$F_c(\theta) = (1 - \alpha_c + \alpha_c\theta_A) \quad (6c)$$

where  $p$  is the probability that group A will react with group B rather than with group C. In these equations  $\alpha_b\theta_A$  means that group B has reacted with A,  $p\alpha_a\theta_B$  that A has reacted with group B, and  $(1 - p)\alpha_a\theta_C$  that A has reacted with group C. The four probabilities  $\alpha_a$ ,  $\alpha_b$ ,  $\alpha_c$ , and  $p$  are not independent. It follows from the condition that A can only react with B or with C

$$\alpha_a = \alpha_b + \alpha_c \quad (7a)$$

$$\alpha_b = p\alpha_a \quad (7b)$$

$$\alpha_c = (1 - p)\alpha_a \quad (7c)$$

Equation 3 is the probability generating function of offspring for all units in the zero generation. For the construction of the first and all other generations one has to take into account that one of the three functionalities A, B, C, is necessarily

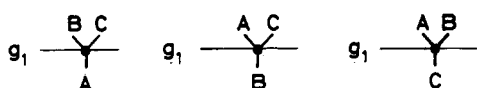


Figure 3. The three possible arrangements of a unit in the first generation and the corresponding generating function for offspring.

linked with a unit of a preceding generation. From graphs of Figure 3 one realizes

$$\begin{aligned} F_{1A}(\theta) &= F_b(\theta)F_c(\theta) \\ F_{1B}(\theta) &= F_a(\theta)F_c(\theta) \\ F_{1C}(\theta) &= F_a(\theta)F_b(\theta) \end{aligned} \quad (8)$$

Insertion of eq 6 into eq 3 and 8 yields the link probability generating functions of the zero generation

$$F_0(\theta) = (1 - \alpha_a + \alpha_b\theta_B + \alpha_c\theta_C) \times (1 - \alpha_b + \alpha_b\theta_A)(1 - \alpha_c + \alpha_c\theta_A) \quad (9)$$

and for the first and all other generations, i.e., for  $n \geq 1$

$$F_{nA}(\theta) = (1 - \alpha_b + \alpha_b\theta_A)(1 - \alpha_c + \alpha_c\theta_A) \quad (10a)$$

$$F_{nB}(\theta) = (1 - \alpha_a + \alpha_b\theta_B + \alpha_c\theta_C)(1 - \alpha_c + \alpha_c\theta_A) \quad (10b)$$

$$F_{nC}(\theta) = (1 - \alpha_a + \alpha_b\theta_B + \alpha_c\theta_C)(1 - \alpha_b + \alpha_b\theta_A) \quad (10c)$$

**Cascade Substitution.** Equations 9 and 10 allow the calculation of the mean number of offspring in each generation. In order to obtain the total population of offspring in all generations the link probability generating functions have to be linked together.

As was shown by Good,<sup>4a</sup> this can be done by a cascade substitution which in the present problem reads

$$U_0(\theta) = \theta^{\phi_0}(1 - \alpha_a + \alpha_b U_{1B} + \alpha_c U_{1C})(1 - \alpha_b + \alpha_b U_{1A})(1 - \alpha_c + \alpha_c U_{1A}) \quad (11)$$

$$U_{nA}(\theta) = \theta^{\phi_n}(1 - \alpha_b + \alpha_b U_{n+1,A})(1 - \alpha_c + \alpha_c U_{n+1,A})$$

$$U_{nB}(\theta) = \theta^{\phi_n}(1 - \alpha_a + \alpha_b U_{n+1,B} + \alpha_c U_{n+1,C})(1 - \alpha_c + \alpha_c U_{n+1,A})$$

$$U_{nC}(\theta) = \theta^{\phi_n}(1 - \alpha_a + \alpha_b U_{n+1,B} + \alpha_c U_{n+1,C})(1 - \alpha_b + \alpha_b U_{n+1,A}) \quad (12)$$

$U_0(\theta)$  is called path weighting generating function and reduces to the simple weight generating function of Good for  $\phi(n) = 1$ . It can be shown that  $U_0$  generates the whole forest mentioned in the section General Considerations. The meaning of the cascade substitution may be elucidated in terms of family trees. It reflects a process where the grandfather is replaced by the father and the father by the son, etc.

Probably  $U_0(\theta)$  cannot be written in an analytic form. Fortunately, this is not necessary and even not desirable. One has to bear in mind that all measurable quantities are averages of the molecular assembly, and these averages can be calculated by differentiating  $U_0(\theta)$  with respect to  $\theta$  and setting  $\theta = 1$ .

As was shown by Kajiwara, Burchard, and Gordon<sup>1</sup> and by Kajiwara and Gordon<sup>9</sup> the differentiation yields

$$\left. \frac{\partial U_0}{\partial \theta} \right|_{\theta=1} = DP_w \quad \text{for } \phi_n = 1 \quad (13a)$$

$$M_w \quad \text{for } \phi_n = M_0 \quad (13b)$$

$$\langle S^2 \rangle_2 2DP_w \quad \text{for } \phi_n = \sigma^2 n \quad (13c)$$

$$P_z(\Theta) DP_w \quad \text{for } \phi_n = \exp(-X^2 n/6) \\ (X^2 = h^2 \sigma^2) \\ = (4\pi^2/\lambda^2) \sin^2 \Theta/2 \quad (13d)$$

On performing the differentiation of  $U_0(\theta)$ , one has to make use of the condition that for all generations

$$U_{nA}(1) = U_{nB}(1) = U_{nC}(1) = 1 \quad (14)$$

Proceeding now from generation to generation, one obtains series which can be factorized into certain sums over infinite series. With some patience but by elementary algebra one finally arrives at (see Appendix I)

$$\begin{aligned} U_0'(1) &= \phi_0 + 2 \sum_{n=1}^{\infty} (\alpha_b + \alpha_c)^{n-1} \phi_n + \\ &2\alpha_b\alpha_c \sum_{k=1}^{\infty} (\alpha_b + \alpha_c)^{n-1} \sum_{n=1}^{\infty} (\alpha_b + \alpha_c)^{n-1} \phi_{n+k} \end{aligned} \quad (15)$$

With the specifications of  $\phi(n)$  from eq 13 one obtains

$$DP_w = \frac{1 - \alpha_b^2 - \alpha_c^2}{(1 - \alpha_b - \alpha_c)^2} \quad (16a)$$

$$M_w = M_0 \frac{1 - \alpha_b^2 - \alpha_c^2}{(1 - \alpha_b - \alpha_c)^2} \quad (16b)$$

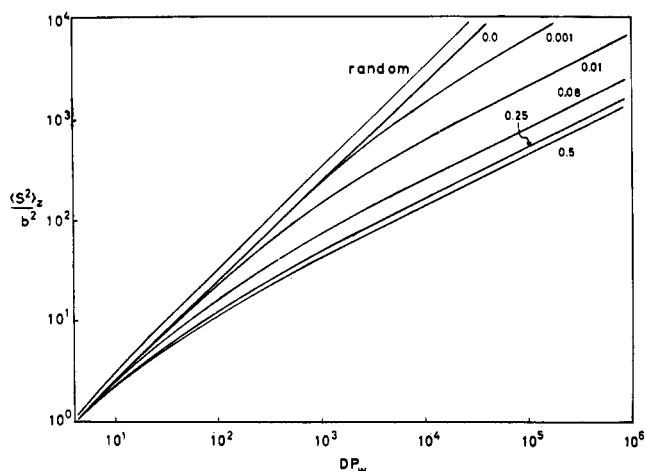


Figure 4. The  $z$  average of the mean square radius of gyration,  $\langle S^2 \rangle_z$ , as function of the weight-average degree of polymerization for several branching values  $\alpha_c$ , in comparison to the random trifunctional polycondensates. The figures at the curves indicate the values of  $\alpha_c$ .

$$\langle S^2 \rangle_z = \sigma^2 \frac{\alpha_b(1 - \alpha_b) + \alpha_c(1 - \alpha_c)}{(1 - \alpha_b^2 - \alpha_c^2)(1 - \alpha_b - \alpha_c)} \quad (16c)$$

$$P_z(\Theta) = \frac{1}{DP_w} \frac{1 - (\alpha_b^2 + \alpha_c^2) \exp(-X^2/3)}{[1 - (\alpha_b + \alpha_c) \exp(-X^2/6)]^2} \quad (16d)$$

The number-average degree of polymerization may be calculated from a general relationship derived by Gordon<sup>5,6</sup>

$$DP_n = \frac{2}{2 - F_0'(1)} = \frac{1}{1 - \alpha_b - \alpha_c} \quad (17)$$

### Computations and Discussion

The equations for the particle scattering factor and the mean-square radius of gyration are instructively discussed in comparison with the properties of the randomly branched trifunctional polycondensates. For this purpose the following previously derived equations are quoted<sup>1</sup>

$$DP_w = \frac{1 + \alpha}{1 - 2\alpha} \quad (18a)$$

$$DP_n = \frac{1}{1 - (3/2)\alpha} \quad (18b)$$

$$\langle S^2 \rangle_z = \sigma^2 \frac{3\alpha}{2(1 + \alpha)(1 - 2\alpha)} \quad (18c)$$

$$P_z(\Theta) = \frac{1}{DP_w} \frac{1 + \alpha \exp(-X^2/6)}{1 - 2\alpha \exp(-X^2/6)} \quad (18d)$$

**The Mean-Square Radius of Gyration as Function of the Degree of Polymerization.** Figure 4 shows the relationship between  $\langle S^2 \rangle_z$  and  $DP_w$  for the random polycondensate and for five cases of the less random Erlander–French type.

As shown elsewhere,<sup>1</sup> the dependence of  $\langle S^2 \rangle_z$  on  $DP_w$  for the random polycondensate approaches quickly the simple relationship

$$\langle S^2 \rangle_z / \sigma^2 \longrightarrow (2/3) DP_w \quad (19)$$

The Erlander–French type condensates, however, exhibit quite different behavior, and may be written (see Appendix II)

$$\langle S^2 \rangle_z / \sigma^2 \longrightarrow [2\alpha_c(1 - \alpha_c)]^{-1/2} DP_w^{1/2} \quad (20a)$$

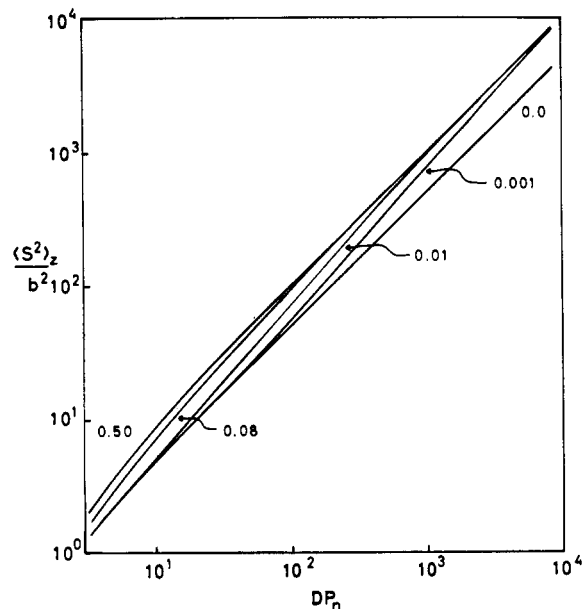


Figure 5.  $\langle S^2 \rangle_z$  dependence on  $DP_n$ . The meaning of the figures is the same as given in Figure 4.

for  $DP_w \gg 1$  and  $\alpha_c \neq \alpha_b$  and

$$\langle S^2 \rangle_z / \sigma^2 \longrightarrow 2^{1/2} DP_w^{1/2} \quad (20b)$$

for  $\alpha_b = \alpha_c$ . If, on the other hand,  $\langle S^2 \rangle_z$  is plotted against  $DP_n$ , a linear relationship is found (Figure 5)

$$\langle S^2 \rangle_z \propto DP_n \quad (21)$$

and follows from eq 16c and 17 by the same argument as given in Appendix II. An asymptote similar to eq 21 does not exist for the random trifunctional polycondensates.

It is worth noticing that the limit of validity for the asymptotes of eq 20 is shifted to higher degrees of polymerization if  $\alpha_c$  deviates considerably from  $\alpha_c = 0.5$ . The reason for this becomes obvious by examining the meaning of  $\alpha_c$ . The reciprocal of the value,  $1/\alpha_c$ , equals the number of monomer units between two branching points and  $\alpha_c = 0$  corresponds therefore to a linear chain. Since for linear chains

$$\langle S^2 \rangle_z / \sigma^2 = \frac{\alpha}{(1 + \alpha)(1 - \alpha)} \cong DP_w = 2DP_n \quad (22)$$

there must occur a continuous transition from the behavior of eq 20a for high  $DP_w$  (where the chain is highly branched) to that of eq 22 for low  $DP_w$  (where the chain essentially is linear).

Thus, for small  $\alpha_c$  values one has to expect a curve in the double logarithmic plot with a variable exponent in the equation

$$\langle S^2 \rangle_z \propto DP_w^\epsilon \quad (0.5 \leq \epsilon \leq 1.0) \quad (23)$$

Such curves are seen in Figure 4 for  $\alpha_c = 0.01$  and  $\alpha_c = 0.001$ . Similar arguments apply for Figure 5.

**The Particle Scattering Factor.** In Figures 6 and 7 the particle scattering factors are compared in Zimm plots, where the abscissa is  $h^2 \langle S^2 \rangle_z$  and  $h = (4\pi/\lambda) \sin \Theta/2$ . The striking feature of these curves is the strong upturn for the different cases of the Erlander–French polycondensation type in contrast to the linear graphs of the random trifunctional and the linear polycondensates. The upturn is most pronounced for  $\alpha_c = \alpha_b$  and becomes more smoothed when  $\alpha_c$  or  $\alpha_b$  is small, and eventually a straight line is obtained when  $\alpha_c$  or  $\alpha_b$

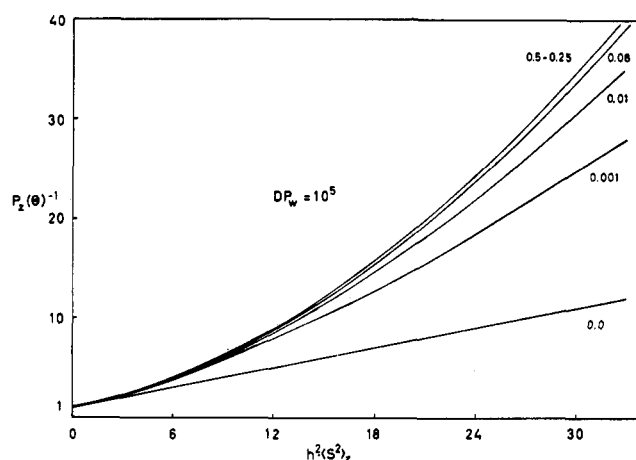


Figure 6. Zimm plots for the particle scattering factors of polymers with  $DP_w = 10^5$ . Meaning of the figures at the curves as in Figure 4.

approaches zero (linear chains). Furthermore, the upturn is less marked for low  $DP_w$  (Figure 7) than for high ones (Figure 6).

This upturn might be expected for branched chains, as it is observed for cruciform molecules.<sup>10</sup> It was therefore surprising that the Zimm plot for the randomly branched polycondensate was found to be linear.<sup>1</sup> This behavior was attributed by Kajiwara, Burchard, and Gordon to the broad molecular weight distribution. The upturn caused by the increase of segment density due to branching appeared to be balanced by the downturn due to the molecular heterogeneity. This interpretation was confirmed by a further paper of Kajiwara,<sup>11</sup> who succeeded in the calculation of the particle scattering factor of homodisperse randomly branched  $f$ -functional polycondensates. The Zimm plots of the particle scattering factors of these products exhibit the expected strong upturn. The upturn which occurs in Zimm plots for the Erlander-French type condensates suggests a narrower molecular weight distribution than for the random case. In fact, Erlander and French showed that the heterogeneity of the type II polycondensates increases approximately with the root of  $DP_w$ , whereas for the random type I polycondensates the heterogeneity varies proportionally to  $DP_w$

$$DP_w/DP_n \propto DP_w^{1/2} \quad \text{for A} \begin{array}{c} \text{B} \\ \diagup \quad \diagdown \\ \text{C} \end{array} \quad (24a)$$

II

$$DP_w/DP_n \propto DP_w \quad \text{for A} \begin{array}{c} \text{A} \\ \diagup \quad \diagdown \\ \text{A} \end{array} \quad (24b)$$

I

The less marked upturn for low  $DP_w$  is naturally explained by the fact that at low  $DP_w$  the chain resembles more and more a linear chain. For instance, at  $DP_w = 10^3$  and  $\alpha_c = 10^{-3}$ , only a few chains have branches, and the corresponding particle scattering factor deviates only slightly from that of a linear chain.

**Length Distribution of Subchains.** It is also of interest to compare the length distribution of subchains within the

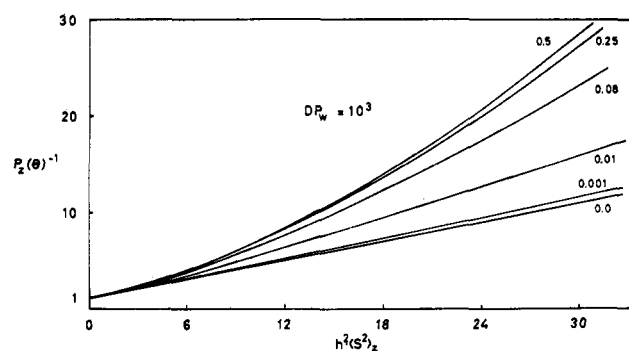


Figure 7. Zimm plots for the particle scattering factors of polymers with  $DP_w = 10^3$ .

branched molecules. This distribution is certainly significant for the behavior of the particle scattering factor, because in the path weighting generating function the contributions of particle scattering factors of all possible subchains are counted and summed. The length distribution for the random type I polycondensation is a most probable distribution<sup>1,4a</sup>

$$h_0(n) = (1 - \alpha)\alpha^{n-1} \quad (25)$$

It is well known that the  $z$  average of  $P(\theta)$  from such a distribution yields a straight line in the Zimm plot, and eq 25 may be regarded as one of the reasons for straight Zimm plots for the randomly branched polycondensates. Following these arguments, one should expect a narrower length distribution for the Erlander-French polycondensation type. This is in fact the case. Applying a method of Good<sup>4a</sup> (see Appendix III) one finds for the length distribution in a type II polycondensate

$$h(n) = \frac{(1 - \alpha_a)^2}{\alpha_a(1 - \alpha_a) + \alpha_b\alpha_c} \{ \alpha_a^n + (n-1)\alpha_b\alpha_c\alpha_a^{n-2} \} \quad (26)$$

This can be written in terms of a most probable and a once convoluted most probable distribution

$$h(n) = \frac{\alpha_a(1 - \alpha_a)h_0(n) + \alpha_b\alpha_ch_{20}(n)}{\alpha_a(1 - \alpha_a) + \alpha_b\alpha_c} \quad (27)$$

where

$$h_{20} = h_0(\alpha_a) * h_0(\alpha_a) = (1 - \alpha_a)^2\alpha_a^{n-2}(n-1) \quad (28)$$

(the asterisk stands for convolution). For high degrees of polymerization the value of  $\alpha_b\alpha_c$  is large compared with  $\alpha_a(1 - \alpha_a)$ , and eq 28 reduces to

$$h(n) \longrightarrow h_{20}(n, \alpha_a) \quad (\alpha_a \cong 1) \quad (29)$$

only, if  $\alpha_c$  is very small, both parts of the linear combination in eq 27 contribute significantly to the length distribution, and in the limit of  $\alpha_c = 0$ , i.e., the linear macromolecule, one has

$$h(n) \longrightarrow h_0(n, \alpha_a) \quad (\alpha_c \rightarrow 0) \quad (30)$$

The narrower distribution (29) may be associated with the upturn of Zimm plots and eq 30 with a linear graph. The change in the upturn on varying  $\alpha_c$  is thereby qualitatively explained.

However, the length distribution of subchains can be only one of two factors, which determine the shape of the particle scattering factor, because convoluted linear chains do not

(10) H. Benoit, *J. Polym. Sci.*, **11**, 507 (1953).

(11) K. Kajiwara, *Polymer*, **12**, 57 (1971).

show such a marked upturn as for the branched chains. A second reason for the upturn must be seen, therefore, in the increase of segment density in the molecule because of branching.

As mentioned in the introduction, the Erlander–French type polycondensate is realized in glycogen and amylopectin. The indicated upturn of the particle scattering factor was indeed observed for some amylopectins.<sup>12,13</sup> Furthermore, as eq 16 is symmetric with respect to  $\alpha_b$  and  $\alpha_c$ , the same theory should also be applicable to dextran. However, in both cases the interpretation of light-scattering data is complicated by a superimposed association of the molecules, and a detailed analysis of the structure of these polysaccharides will be given elsewhere.

**Acknowledgment.** The essential part of this paper was developed during the author's stay at Essex University, Colchester, England, in 1968–1969. The author wishes to thank Professor M. Gordon for his hospitality, many discussions, and encouragements. He also thanks his colleague Dr. K. Kajiwara (Freiburg) for discussions and the Royal Society of London and the Deutsche Forschungsgemeinschaft for a joint grant.

#### Appendix I. Derivation of Eq 15

The path weighting generating function is written

$$\begin{aligned} U_0(\theta) &= \theta^{\phi_0}(1 - \alpha_a + \alpha_b U_{1,B} + \alpha_c U_{1,C}) \times \\ &\quad (1 - \alpha_b + \alpha_b U_{1,A})(1 - \alpha_c + \alpha_c U_{1,A}) \\ U_{n,A}(\theta) &= \theta^{\phi_n}(1 - \alpha_b + \alpha_b U_{n+1,A}) \times \\ &\quad (1 - \alpha_c + \alpha_c U_{n+1,A}) \\ U_{n,B}(\theta) &= \theta^{\phi_n}(1 - \alpha_a + \alpha_b U_{n+1,B} + \alpha_c U_{n+1,C}) \times \\ &\quad (1 - \alpha_c + \alpha_c U_{n+1,A}) \\ U_{n,C}(\theta) &= \theta^{\phi_n}(1 - \alpha_a + \alpha_b U_{n+1,B} + \alpha_c U_{n+1,C}) \times \\ &\quad (1 - \alpha_b + \alpha_b U_{n+1,A}) \quad (A1) \end{aligned}$$

Differentiation at  $\theta = 1$  yields

$$U_0'(1) = \phi_0 + \alpha_b U_{1,B}' + \alpha_c U_{1,C}' + (\alpha_b + \alpha_c) U_{1,A}' \quad (A2)$$

with recursion formulas

$$\begin{aligned} U_{n,A}'(1) &= \phi_n + (\alpha_b + \alpha_c) U_{n+1,A}' \\ U_{n,B}'(1) &= \phi_n + \alpha_b U_{n+1,B}' + \alpha_c U_{n+1,C}' + \alpha_c U_{n+1,A}' \\ U_{n,C}'(1) &= \phi_n + \alpha_b U_{n+1,B}' + \alpha_c U_{n+1,C}' + \alpha_b U_{n+1,A}' \quad (A3) \end{aligned}$$

Starting with  $n = 1$  one obtains for

$$\begin{aligned} U_{1,A} &= \phi_1 + (\alpha_b + \alpha_c) U_{2,A}' \\ &= \phi_1 + (\alpha_b + \alpha_c) \phi_2 + (\alpha_b + \alpha_c)^2 U_{3,A}' \\ &= \phi_1 + (\alpha_b + \alpha_c) \phi_2 + (\alpha_b + \alpha_c)^2 \phi_3 + \dots + \\ &\quad (\alpha_b + \alpha_c)^{n-1} U_{n,A}' \end{aligned}$$

This can be summarized as

$$U_{1,A}' = \sum_{n=1}^{\infty} (\alpha_b + \alpha_c)^{n-1} \phi_n \quad (A4)$$

Similarly, one finds for

$$\begin{aligned} U_{1,B}' &= \phi_1 + \alpha_b U_{2,B}' + \alpha_c U_{2,C}' + \alpha_c U_{2,A}' \\ &= \phi_1 + (\alpha_b + \alpha_c) \phi_2 + (\alpha_b + \alpha_c) [\alpha_b U_{3,B}' + \\ &\quad \alpha_c U_{3,C}'] + \alpha_c U_{2,A}' + 2\alpha_b \alpha_c U_{3,A}' \\ U_{1,B}' &= \sum_{n=1}^{\infty} (\alpha_b + \alpha_c)^{n-1} \phi_n + \alpha_c U_{2,A}' + \\ &\quad 2\alpha_b \alpha_c \sum_{n=1}^{\infty} (\alpha_b + \alpha_c)^{n-1} U_{n+2,A}' \quad (A5) \end{aligned}$$

and since

$$U_{k,A}' = \sum_{n=1}^{\infty} (\alpha_b + \alpha_c)^{n-1} \phi_{n+k-1} \quad (A6)$$

one obtains

$$\begin{aligned} U_{1,B}' &= \sum_{n=1}^{\infty} (\alpha_b + \alpha_c)^{n-1} \phi_n + \alpha_c \sum_{n=1}^{\infty} (\alpha_b + \alpha_c)^{n-1} \phi_{n+1} + \\ &\quad 2\alpha_b \alpha_c \sum_{n=1}^{\infty} (\alpha_b + \alpha_c)^{n-1} \sum_{k=1}^{\infty} (\alpha_b + \alpha_c)^{k-1} \phi_{n+k-1} \quad (A7) \end{aligned}$$

A very similar result is found for  $U_{1,C}'$

$$\begin{aligned} U_{1,C}' &= \sum_{n=1}^{\infty} (\alpha_b + \alpha_c)^{n-1} \phi_n + \alpha_b \sum_{n=1}^{\infty} (\alpha_b + \alpha_c)^{n-1} \phi_{n+1} + \\ &\quad 2\alpha_b \alpha_c \sum_{n=1}^{\infty} (\alpha_b + \alpha_c)^{n-1} \sum_{k=1}^{\infty} (\alpha_b + \alpha_c)^{k-1} \phi_{n+k-1} \quad (A8) \end{aligned}$$

Insertion of (A4), (A7), and (A8) into (A2) yields

$$\begin{aligned} U_0'(1) &= \phi_0 + 2(\alpha_b + \alpha_c) \sum_{n=1}^{\infty} (\alpha_b + \alpha_c)^{n-1} \phi_n + \\ &\quad 2\alpha_b \alpha_c \sum_{n=1}^{\infty} (\alpha_b + \alpha_c)^{n-1} \sum_{k=1}^{\infty} (\alpha_b + \alpha_c)^{k-1} \phi_{n+k} \end{aligned}$$

which is the result of eq 15 in the text.

#### Appendix II. Behavior of $\langle S^2 \rangle_z$ at Large $DP_w$

Equation 16 may be written as

$$\frac{\langle S^2 \rangle_z}{\sigma^2} = \frac{\alpha_b(1 - \alpha_b) + \alpha_c(1 - \alpha_c)}{(1 - \alpha_b^2 - \alpha_c^2)^{3/2}} DP_w^{1/2} \quad (A9)$$

On solving eq 16a for  $\alpha_b$  one obtains

$$\begin{aligned} \alpha_b &= (1 - \alpha_c) \frac{DP_w}{1 + DP_w} \pm (1 - \alpha_c) \left[ \left( \frac{DP_w}{1 + DP_w} \right)^2 - \right. \\ &\quad \left. \frac{DP_w}{1 + DP_w} + \frac{1}{1 + DP_w} \frac{1 + \alpha_c}{1 - \alpha_c} \right]^{1/2} \quad (A10) \end{aligned}$$

In the limit of large  $DP_w$

$$\frac{DP_w}{1 + DP_w} \rightarrow 1; \quad \frac{1}{1 + DP_w} \rightarrow 0$$

thus

$$\alpha_b \cong 1 - \alpha_c \quad (A11)$$

Insertion of  $\alpha_b$  into eq A9 yields eq 20a of the text. Finally, if  $\alpha_b = \alpha_c$  and  $DP_w \gg 1$ , the probability  $\alpha_b$  approaches the limiting value 0.50 and eq 20b follows then from (20a).

#### Appendix III. Length Distribution of Subchains

According to Good,<sup>4a</sup> the generating function for the number of offspring in the  $n$ th generation is found by the following cascade substitution

$$G = F_0(F_1(F_2(\dots F_{n-1}(\dots))) \quad (A12)$$

(12) C. J. Stacy and J. Foster, *J. Polym. Sci.*, **20**, 57 (1956).

(13) S. R. Erlander and D. French, *ibid.*, **32**, 291 (1958).

where  $F_0$  is given by eq 9 of the text and

$$\mathbf{F}_j = (F_{jA}, F_{jB}, F_{jC}) \quad j = 1, 2, \dots \quad (\text{A13})$$

with components  $F_{jA}$ ,  $F_{jB}$ , and  $F_{jC}$  as defined in eq 10. More explicitly, eq A12 reads

$$G(\theta) = (1 - \alpha_a + \alpha_b G_{1,B} + \alpha_c G_{1,C}) \times \\ (1 - \alpha_b + \alpha_b G_{1,A})(1 - \alpha_c + \alpha_c G_{1,A}) \quad (\text{A14})$$

$$G_{j,A} = (1 - \alpha_b + \alpha_b G_{j+1,A})(1 - \alpha_c + \alpha_c G_{j+1,A})$$

$$G_{j,B} = (1 - \alpha_a + \alpha_b G_{j+1,B} + \alpha_c G_{j+1,C}) \times \\ (1 - \alpha_c + \alpha_c G_{j+1,A})$$

$$G_{j,C} = (1 - \alpha_a + \alpha_b G_{j+1,B} + \alpha_c G_{j+1,C}) \times \\ (1 - \alpha_b + \alpha_b G_{j+1,A}) \quad (\text{A15})$$

(for  $j < n - 1$ )

$$G_{n-1,A} = (1 - \alpha_b + \alpha_b \theta)(1 - \alpha_c + \alpha_c \theta)$$

$$G_{n-1,B} = (1 - \alpha_a + [\alpha_b + \alpha_c]\theta)(1 - \alpha_c + \alpha_c \theta)$$

$$G_{n-1,C} = (1 - \alpha_a + [\alpha_b + \alpha_c]\theta)(1 - \alpha_b + \alpha_b \theta) \quad (\text{A16})$$

Again the average number of offspring is obtained by differentiation at  $\theta = 1$ . This yields

$$G'(1) = \alpha_b G_{1,B}' + \alpha_c G_{1,C}' + (\alpha_b + \alpha_c) G_{1,A}' \quad (\text{A17})$$

The value for  $G_{1,A}'$  results immediately for the first lines of (A15) and (A16)

$$G_{1,A}' = (\alpha_b + \alpha_c)^{n-1} \quad (\text{A18})$$

The evaluation of  $G_{1,B}'$  and  $G_{1,C}'$  is more involved. After some rearrangements one obtains

$$\alpha_b G_{1,B}' + \alpha_c G_{1,C}' = (\alpha_b + \alpha_c)^n + \\ 2(n-1)\alpha_b\alpha_c(\alpha_b + \alpha_c)^{n-2} \quad (\text{A19})$$

Inserting (A18) and (A19) into (A17) one finds the average number of offspring in the  $n$ -th generation  $\langle N \rangle_n$

$$\langle N \rangle_n = 2(\alpha_b + \alpha_c)^n + 2(n-1)\alpha_b\alpha_c(\alpha_b + \alpha_c)^{n-2} \quad (\text{A20})$$

Since the number of nodes in the  $n$ -th generation equals the number of paths of length  $n$  from the zero-th generation, the normalized path-length distribution is

$$h(n) = \frac{(1 - \alpha_a)^2}{\alpha_a(1 - \alpha_a) + \alpha_b\alpha_c} \{ \alpha_a^n + \alpha_b\alpha_c\alpha_a^{n-2} \} \quad (\text{A21})$$

where

$$\alpha_a = \alpha_b + \alpha_c$$

## Small-Angle Light Scattering of Reconstituted Collagen<sup>1</sup>

James C. W. Chien\* and E. P. Chang

Department of Chemistry and the Polymer Research Institute of the

University of Massachusetts, Amherst, Massachusetts 01002. Received April 21, 1972

**ABSTRACT:** Small-angle light scattering of reconstituted collagen films was photographed with  $H_V$ ,  $V_V$ ,  $V_H$ ,  $H_H$ , and intermediate configurations, where H and V refer to the direction of electric vector of the analyzer and the subscript denotes the polarizer direction. The effects of temperature, swelling, and deformation in the superstructures can be followed by observing changes in SALS. A deformation mechanism is presented detailing the various stages of strain-induced orientation. Cross-linked collagen film appears to contain smaller size scattering elements, which are more susceptible to orientation by swelling and temperature changes than those films which have not been irradiated. Films of collagen-poly(vinyl alcohol) copolymer gave SALS patterns nearly the same as the collagen homopolymer films. The grafted poly(vinyl alcohol), however, does not form new superstructural units, and it tends to plasticize the collagen units. Under high strain the molecules in reconstituted collagen film rearrange to form incipient "native" fibrils; the copolymer samples do not do so. When the sample is highly oriented, the polarized laser beam passing through it becomes depolarized. Light and phase contrast microscopy were also used to verify some of the SALS conclusions.

It is generally accepted that the basic constituent of collagenous substance is the tropocollagen triple-helical molecule which is about 3000 Å in length and 15 Å in diameter.<sup>2</sup> They aggregate in a solid state forming quarter staggered, fibrous long-spacing,<sup>3a</sup> or segment long-spacing<sup>3b</sup> crystallites. These in turn are assembled into long parallel bundles of fibrils such as those in rattail tendon. They are laid down in mutually perpendicular layers in the cornea. Therefore, there are several levels of superstructures, all having dimensions comparable to the wavelength of light. They

should scatter light efficiently as anisotropic rods or disks. A theory for the angular dependence of light scattering by a random assembly of such entities in two dimensions has been formulated by Stein and Rhodes.<sup>4</sup> This theory has been widely used in the interpretation of small-angle light-scattering (SALS) patterns. Recently, Kawai, *et al.*,<sup>5</sup> reported some SALS patterns obtained with films of acid-soluble collagen and enzyme-solubilized collagen. The conventional  $H_V$  and  $V_V$  configurations were used (the subscript designates that the electric vector of the polarizer is vertical, the letters H and V indicate the directions of the electric vectors of the analyzer). The fourfold symmetrical  $H_V$  pattern was found to be the (+)

(1) Presented in part at the American Physical Society Meeting, March 29, 1972, Atlantic City, N. J.

(2) H. Boedtker and P. J. Doty, *J. Amer. Chem. Soc.*, **78**, 4267 (1956).

(3) (a) J. H. Highberger, J. Gross, and F. O. Schmitt, *ibid.*, **72**, 3321 (1950); *Proc. Nat. Acad. Sci. U. S.*, **37**, 286 (1951); (b) F. O. Schmitt, J. Gross, and J. H. Highberger, *J. Exptl. Cell. Res., Suppl.*, **3**, 326 (1955).

(4) R. S. Stein and M. B. Rhodes, *J. Appl. Phys.*, **31**, 1873 (1960).

(5) M. Moritani, N. Hayashi, A. Utsuo, and H. Kawai, *Polym. J.*, **2**, 74 (1971).